
Mitigating Object Hallucination via Concentric Causal Attention

Yun Xing^{1*} Yiheng Li^{1*} Ivan Laptev² Shijian Lu^{1†}

¹ Nanyang Technological University ² MBZUAI

<https://github.com/xing0047/cca-llava.git>

Abstract

Recent Large Vision Language Models (LVLMs) present remarkable zero-shot conversational and reasoning capabilities given multimodal queries. Nevertheless, they suffer from object hallucination, a phenomenon where LVLMs are prone to generate textual responses not factually aligned with image inputs. Our pilot study reveals that object hallucination is closely tied with Rotary Position Encoding (RoPE), a widely adopted positional dependency modeling design in existing LVLMs. Due to the long-term decay in RoPE, LVLMs tend to hallucinate more when relevant visual cues are distant from instruction tokens in the multimodal input sequence. Additionally, we observe a similar effect when reversing the sequential order of visual tokens during multimodal alignment. Our tests indicate that long-term decay in RoPE poses challenges to LVLMs while capturing visual-instruction interactions across long distances. We propose Concentric Causal Attention (CCA), a simple yet effective positional alignment strategy that mitigates the impact of RoPE long-term decay in LVLMs by naturally reducing relative distance between visual and instruction tokens. With CCA, visual tokens can better interact with instruction tokens, thereby enhancing model’s perception capability and alleviating object hallucination. Without bells and whistles, our positional alignment method surpasses existing hallucination mitigation strategies by large margins on multiple object hallucination benchmarks.

1 Introduction

Large Vision-Language Models (LVLMs) [46, 45, 84, 71, 6, 15, 5] have drawn increasing attention from the AI research community due to their impressive power in understanding the visual world and unprecedented ability to interact with humans via conversations. Their capability to process multimodal sequences has opened up new possibilities for a wide range of vision and language tasks [32, 2], such as handling interleaved image-text inputs [4, 35] and interactive user queries [82]. However, existing LVLMs still suffer from object hallucination [57, 41, 44, 14], a tendency to generate inaccurate responses that are not factually aligned with image inputs. Such phenomenon challenges the faithfulness and reliability of LVLMs in practical use, impeding their deployments to real-world applications [14].

A wide range of approaches have been proposed to mitigate object hallucination in LVLMs. One straightforward approach involves post-hoc correction using revisor models [73, 83], reducing occurrences of hallucinated responses. Another viable approach is to improve supervised fine-tuning by diversifying instruction tuning data [43] or additionally aligning model responses with human preference [62, 76]. Despite their effectiveness in mitigating LVLM object hallucination, acquiring high-quality annotations can be labor-intensive, making these approaches costly to implement.

^{*}Equal contribution

[†]Corresponding author

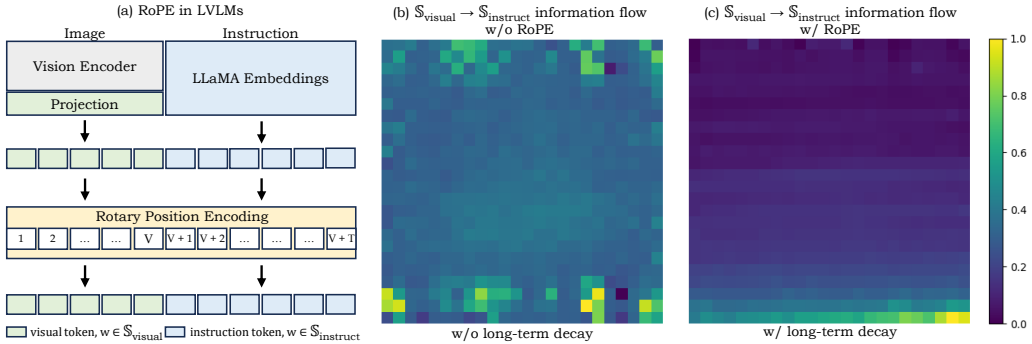


Figure 1: Long-term decay of RoPE [61] in Large Vision Language Models (LVLMs). (a) a schematic view of inference in LVLMs, typically involving a pre-trained vision encoder, a large language model and a projector to map visual tokens to textual space. For each of V visual tokens $\mathbb{S}_{\text{vision}}$, we aggregate its information flow to instruction tokens $\mathbb{S}_{\text{instruct}}$ and reshape the aggregation results to 2-D (\sqrt{V} by \sqrt{V}). Applying RoPE on visual tokens introduces long-term decay as illustrated in (c), referring to the phenomenon where information flowing from visual tokens to instruction tokens gradually decays from lower-right region (rightmost visual tokens in the 1-D sequence) to upper-left region (leftmost visual tokens). For instruction tokens, they have much less direct interaction with leftmost visual tokens as compared with rightmost visual tokens, leading to inferior multimodal alignment in the trained LVLMs. (b) and (c) are derived from the adversarial subset of the 3k POPE [41] image-instruction pairs. Best viewed in color.

Recently, several studies explore training-free mitigation of object hallucination by rectifying fallacies in LVLM autoregressive decoding [26, 34]. However, the need to compare among many candidates inevitably slows down the decoding process, making these approaches less efficient during inference.

Distinct from previous efforts, we attend to Rotary Position Encoding (RoPE) [61], a widely used positional dependency modeling design in LVLMs [46, 84], and investigate how it may affect object hallucination in LVLMs. Similar to sinusoidal function [65], RoPE is proposed to encode position information into representations, enhancing model’s ability in understanding sequential order of input tokens. In spite of its success in modeling natural language [53, 63, 64], this design leads to long-term decay [61] in multimodal alignment, a phenomenon where information flow from visual tokens to instruction tokens¹ gradually diminishes with increasing relative distance.

We analyze the impact of long-term decay [61, 53] on LVLMs. For every visual token in a multimodal sequence, we aggregate its information flow to all instruction tokens and examine how these aggregations distribute across all visual tokens. As presented, in contrast to information flows of visual tokens without RoPE (Fig. 1, (b)), applying RoPE attenuates information flows of leftmost visual tokens, which are located the farthest from instruction tokens in the sequence (Fig. 1, (c)). Such long-term decay benefits natural language modeling [61], but induces insufficient interactions between visual tokens and instruction tokens, leading to inferior multimodal alignment and object hallucinations in the trained LVLMs (see our experiments in Sec. 3 for details).

To this end, we propose Concentric Causal Attention (CCA), a novel position alignment method for training LVLMs with mitigated object hallucination. CCA consists of a position reorganization module for visual tokens and an accompanying causal mask rectification module for modeling 2-D continuous positional dependency. Instead of following raster-scan² sequential order of existing LVLMs, CCA starts from peripheral of 2-D images and ends in centers. Such position alignment strategy enjoys two merits: 1) relative distance from instruction tokens to visual tokens are significantly reduced, alleviating limitations brought by long-term decay in RoPE; 2) rectified causal attentions follow 2-D spatial locality of images, as compared to 1-D causal attention originally designed for natural languages. We carry out pre-training and instruction tuning as [46] and verify our trained model on multiple object hallucination benchmarks [41, 57, 20] (+4.24% on Accuracy and +2.73% on F1 score, as compared to the state-of-the-art method [34] on POPE). From a broader perspec-

¹Information flow here refers to self-attentions from instruction tokens to visual tokens.

²2-D image tokens are flattened from left to right, top to bottom, into 1-D visual token sequence.

tive, our method also improves general perception capability of LVLMs. Preliminary experiments show that our positional alignment approach surpasses the baseline consistently over 6 multimodal benchmarks [36, 48, 22, 28, 49, 8].

Our contributions are three-fold. First, we perform in-depth analysis on correlation between rotary position encoding and object hallucination in large vision-language models. Second, motivated by our analysis, we propose Concentric Causal Attention (CCA), a simple yet effective method to mitigate LVLM object hallucination caused by RoPE long-term decay. Third, experiments on multiple benchmarks and comparisons with the state-of-the-art methods support efficacy of our design.

2 Related Works

Large Vision Language Models. Language modeling has made notable progress in recent years, evolving from robust representation models [17, 56, 55] to instruction-tuned conversational chatbots [63, 64, 12, 1]. These achievements have driven research in creating Large Vision Language Models (LVLMs) that can manage multimodal inputs [72, 46, 45, 84, 71, 6, 67, 40, 51, 39]. Pioneering studies in this field [2, 4, 38, 37] connect a vision-only encoder with a powerful frozen language-only model to bridge modality gap, enabling dense interactions across visual and textual features. Powered by instruction-tuned LLMs [12], LLaVA [46], InstructBLIP [15] and MiniGPT4 [84] allow interactive conversations between trained models and users. On top of these studies, LVLMs are empowered with more advanced capabilities, such as engaging in referential dialogues [7, 74, 81, 54, 77], handling interleaved image-text data [2, 4, 35] or understanding visual prompts, like point or box inputs from users [54, 82, 9, 77]. Despite advancements in LVLMs, many of these models still generate inaccurate responses not aligned with visual inputs.

Object Hallucination refers to a common problem of existing LVLMs [14, 44, 21, 41, 68, 52, 3, 19, 66]. Specifically, LVLMs tend to generate inaccurate responses that are not factually aligned with image inputs. To address this issue, several recent explorations [73, 83, 33] resort to post-hoc correction of model hallucinated outputs. These methods rely on either external models [47] to correct hallucinated responses [73] or on self-correction techniques [33, 70]. However, both of these methods break end-to-end inference scheme. In contrast, [43, 76, 62, 29, 78, 75] ground their approaches on improving instruction tuning, by either diversifying instruction data or aligning model responses with human feedback. However, acquisition of more instruction data or preference data is labor-intensive. Recently, several studies attempt to mitigate object hallucination in a training-free manner [26, 34, 10]. However, the need to compare among many candidates inevitably slows down the decoding process, making these approaches less efficient during inference. From a distinct perspective, we ground our design in correlation between widely adopted rotary position encoding and object hallucination.

Position Encoding in Transformers. Transformer models [65] do not inherently comprehend sequential information of input tokens, which is inferior for modeling sequential data like natural language as compared to recurrent structures like [24]. To mitigate this issue, [65] introduces sinusoidal position encodings to incorporate position information to input embeddings. In addition, several studies resort to learnable position encodings [18], which allow their models to update positional parameters during training. In contrast to absolute position encodings, relative position encodings [59, 31, 23, 27] focus on relative position among tokens. They integrate position information in self-attentions, presenting potential for modeling sequences with variable lengths [61, 53]. Among these studies, Rotary Position Encoding (RoPE) [61] encodes position information by multiplying input embeddings with rotation matrices. In comparison to other position encoding designs, RoPE is capable of equipping linear self-attention with relative position encoding, which is proven effective for pre-training large language models [63, 64]. A few recent studies explores RoPE for vision tasks [13, 50, 69], showcasing its potential to domains beyond natural language. In this paper, we investigate the role of RoPE in LVLMs and how it affects object hallucination in these models.

3 Motivation

In this section, we further examine the long-term decay in RoPE and conduct quantitative analyses to illustrate its correlation with object hallucination. We begin with a brief introduction to the widely adopted LVLM architecture and how RoPE [61] is applied in LVLMs. Then, we highlight the long-term decay in RoPE [61, 53], which benefits language modeling but is under-explored for

multimodal alignment. Finally, we examine the role of RoPE in LVLM object hallucination through comparative experiments, which forms a strong foundation of our design.

LVLM. Typically, an LVLM \mathcal{F} is composed of a pretrained vision encoder \mathcal{F}_v , a large language model \mathcal{F}_t and a projector module f that maps visual embeddings to textual space. Given an image input I_v and instruction input I_t (e.g., “*please describe this image in detail*”), \mathcal{F} encodes these two inputs into a multimodal sequence $\mathbb{S} = \{\mathbb{S}_{vision}, \mathbb{S}_{instruct}\}$, where $\mathbb{S}_{vision} = f(\mathcal{F}_v(I_v)) = \{w_m\}_{m=1}^V$ and $\mathbb{S}_{instruct} = \mathcal{F}_t(I_t) = \{w_m\}_{m=1}^T$ represent visual and instruction tokens of lengths V and T , respectively. In such sequence, visual and instruction tokens share the same dimension d , noted as $w_m \in \mathbb{R}^d$.

Rotary Position Encoding in LVLM. In LLMs like LLaMA [63] and its multimodal successors, RoPE [61] encodes position information with input tokens by multiplying every token w_m with a rotation matrix $R_{\theta,m}^d$,

$$R_{\theta,m}^d = \begin{pmatrix} \cos m\theta_1 & -\sin m\theta_1 & 0 & 0 & \cdots & 0 & 0 \\ \sin m\theta_1 & \cos m\theta_1 & 0 & 0 & \cdots & 0 & 0 \\ 0 & 0 & \cos m\theta_2 & -\sin m\theta_2 & \cdots & 0 & 0 \\ 0 & 0 & \sin m\theta_2 & \cos m\theta_2 & \cdots & 0 & 0 \\ \vdots & \vdots & \vdots & \vdots & \ddots & \vdots & \vdots \\ 0 & 0 & 0 & 0 & \cdots & \cos m\theta_{d/2} & -\sin m\theta_{d/2} \\ 0 & 0 & 0 & 0 & \cdots & \sin m\theta_{d/2} & \cos m\theta_{d/2} \end{pmatrix} \quad (1)$$

where $m \in [1, \dots, V + T]$ indicates position of input token w_m and $\{\theta_i = 10000^{-2(i-1)/d}\}, i \in [1, 2, \dots, d/2]$ are pre-defined sinusoidal function values following [65]. In LVLMs like LLaVA [46], rotary matrices $R_{\theta,m}^d$ are applied to query and key tokens in all decoder layers, such that relative position dependency among tokens are modeled and integrated in self-attentions across the network. In comparison to absolute position encodings [65] and learnable position encodings in ViT [18], RoPE captures relative distance among input tokens and has the potential to extend the input context window beyond a fixed length [53].

RoPE Long-term Decay. Assume a query token q_i at position i and a key token k_j at position j , which are derived from input tokens w_i, w_j . The self attention $a_{i,j}$ between tokens q_i and k_j can be calculated via

$$a_{i,j} = \text{softmax}\left(\frac{q_i^T \cdot k_j}{\sqrt{d}}\right) \quad (2)$$

RoPE applies rotation matrix $R_{\theta,m}^d$ to the self-attention above, which is in the form of,

$$a_{i,j} = \text{softmax}\left(\frac{q_i^T \cdot (R_{\theta,i}^d)^T \cdot R_{\theta,j}^d \cdot k_j}{\sqrt{d}}\right) = \text{softmax}\left(\frac{q_i^T \cdot R_{\theta,j-i}^d \cdot k_j}{\sqrt{d}}\right) \quad (3)$$

where $j - i$ stands for relative position between q_i and k_j . The long-term decay refers to the decrease of $a_{i,j}$ as the relative distance $j - i$ increases. As presented in Fig. 1 (c), visual-to-instruction information flow (i.e., instruction-to-visual self-attention) is less significant when $j - i$ is large and vice versa.

This is favorable for pre-trained LLMs like LLaMA [63], as it aligns with language modeling intuition: pairs of tokens with a long relative distance should have weaker connection. However, we observe that this property brings negative effect in multimodal alignment, in which case visual tokens far from instructions are less attended. This is not expected for multimodal alignment, as the connection between instruction tokens and visual tokens should not be attenuated by their relative distances.

Pilot Experiment. We quantitatively examine the effect of RoPE long-term decay on LVLM object hallucination. To determine how object hallucination is influenced by the distance between visual and instruction tokens, we first train two LVLMs³ following [46] with two different position alignment strategies, including:

³Training details for these two models are in Appendix C.1.

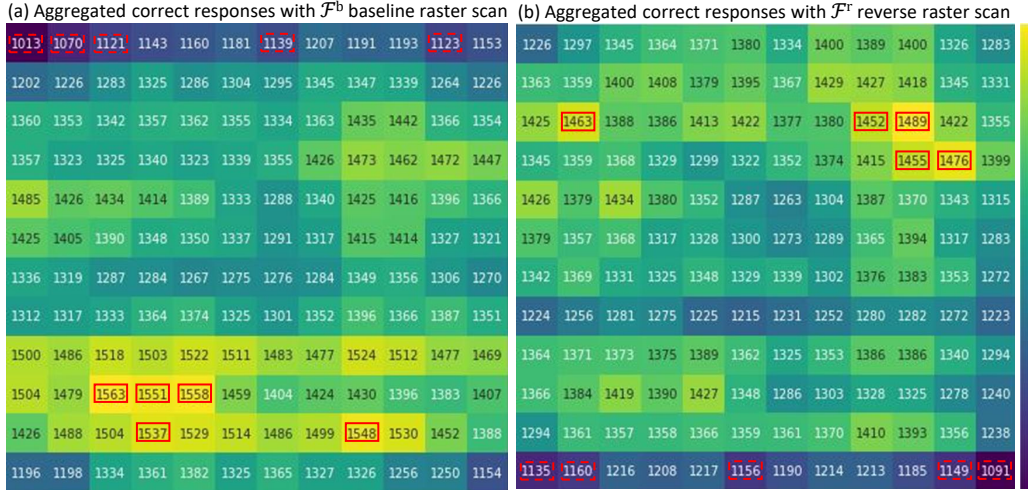


Figure 2: **Motivation Experiment.** Given an image I_v with object O_v , we crop O_v and paste it to various spatial positions $\{v_1, \dots, v_k\}$ within a pre-defined template. For every pasting position, we ask two LVLMs (\mathcal{F}_b and \mathcal{F}_r) if object O_v is in this template, where \mathcal{F}_b refers to a baseline model that follows raster-scan positional alignment strategy and \mathcal{F}_r refers to a model that resorts to reversal raster-scan position alignment strategy. The total number of correct responses at different pasting positions $\{v_1, \dots, v_k\}$ is reported in (a) and (b), which refers to results from model \mathcal{F}_b and \mathcal{F}_r , respectively. We observe that LVLML \mathcal{F}_b are more likely to generate correct responses when pasting object O_v to lower region, while \mathcal{F}_r are less hallucinated when pasting object O_v to upper region. Pasting positions with the most and the least correct responses are highlighted in solid-line and dotted-line red boxes. More details are provided in Appendix C.1. Best viewed in color.

- \mathcal{F}^b (*raster-scan*): it follows [46] the position alignment strategy on visual tokens \mathbb{S}_{vision} . Under this scenario, visual tokens follow a sequential order, starting from upper-left corner to lower-right corner of input 2-D visual features, row by row. The order of a multimodal sequence \mathbb{S} is in format of $\{1, 2, \dots, V, V + 1, \dots, V + T\}$.⁴
- \mathcal{F}^r (*reverse raster-scan*): it reverses the sequential order of visual tokens \mathbb{S}_{vision} . In this case, sequence order of visual tokens starts from lower-right corner of input 2-D visual features to upper-left corner, row by row. The order of full multimodal sequence \mathbb{S} is in format of $\{V, V - 1, \dots, 1, V + 1, \dots, V + T\}$.

The *reverse raster-scan* model \mathcal{F}^r alters relative positions between visual tokens \mathbb{S}_{vision} and instruction tokens $\mathbb{S}_{instruct}$. For example, for instruction token w_{V+1} , its relative distance to visual token w_V changes from 1 to V , resulting in weaker correlations between w_V and w_{V+1} .

Our experiment setup is as follows. Given an image I_v , we follow [41] and ask questions in a polling-base manner. Specifically, for an object O_v in image I_v , we follow the instruction format of “is there a/an {object} in this image?” to test our models. We crop region of object O_v from I_v according to its bounding box annotation and paste the cropped object over different positions of a pre-defined image template (more details are covered in Appendix C.1). This results in new images $\{I_{v_1}, \dots, I_{v_k}\}$, where $\{v_1, \dots, v_k\}$ indicates different pasting positions. We carry out these testing over N images from [42] and aggregate correct responses with respect to pasting positions $\{v_1, \dots, v_k\}$.

RoPE affects object hallucination. The quantitative results of model \mathcal{F}^b and \mathcal{F}^r are visualized in Fig. 2 (a) and (b), respectively. For model \mathcal{F}^b , we find that the response is less likely correct when object O_v is pasted on the upper part of the image, and it is more likely correct when object O_v is pasted on the lower part of image template. This is in stark contrast to \mathcal{F}^r experimental results: model responses are more likely to be correct when pasting image crop O_v on the upper part of images, while less likely to be correct when pasting position is the lower part. For model \mathcal{F}^r , we note

⁴For demonstration purpose, we assume visual tokens are pre-pended before instruction tokens. For implementation, we adapt our design for flexible structure of multimodal sequences.

that visual tokens of lower part is far from instruction tokens in relative distance, corresponding to worse performance in object hallucination. We can thus conclude that RoPE long-term decay affects object hallucination for LVLMs, which requires special care to mitigate this issue.

4 Concentric Causal Attention

To this end, we introduce Concentric Causal Attention, a simple position alignment strategy that mitigates object hallucination by tackling the long-term decay issue originated from RoPE. Our methodology is guided by two key principles,

- Alleviate the effect of long term decay on object hallucination by minimising overall relative distance between visual tokens \mathbb{S}_{vision} and instruction tokens $\mathbb{S}_{instruct}$.
- Mitigate performance discrepancy between *raster scan* model \mathcal{F}^b and *reverse raster scan* model \mathcal{F}^r .

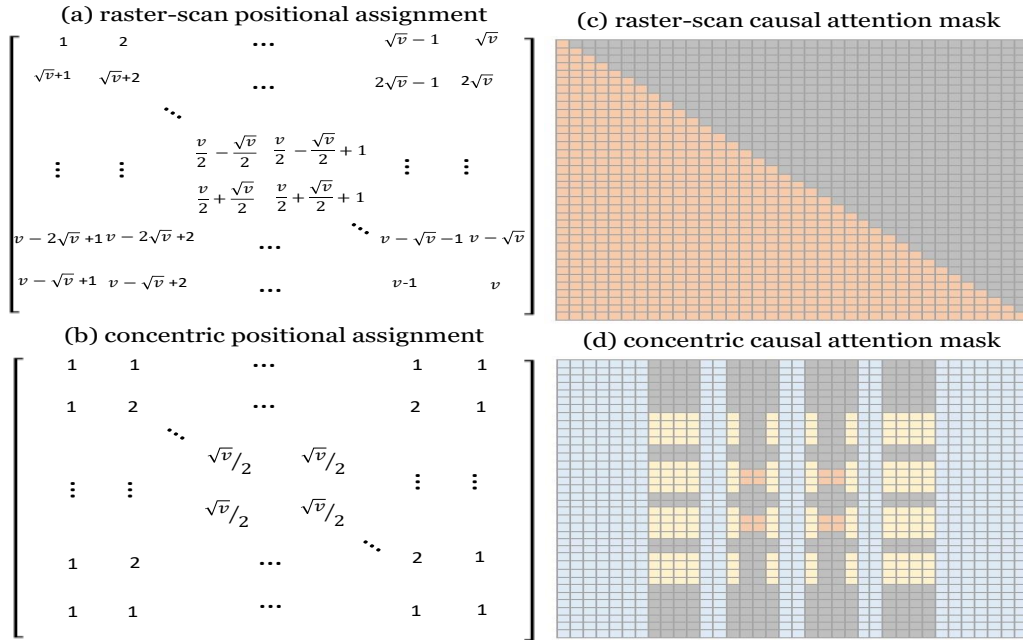


Figure 3: An overview for Concentric Causal Attention. **Left: Visual Token Re-organization.** In comparison to *raster-scan positional alignment* in (a), we design *concentric position alignment* in (b) which shortens visual-instruction distance and retains spatial locality for 2-D data like images. **Right: Concentric Causal Masking.** By default as in (c), a visual token attends to all preceding visual tokens in a 1-D sequence. In contrast, our *concentric causal attention* in (d) models 2-D continuous positional dependencies among visual tokens, where center visual tokens attend to peripheral ones. Causal masks are V by V where in this case V is 36 for demonstration purpose. Best viewed in color.

Concentric Positions. In existing LVLMs such as LLaVA [46], visual tokens are perceived in 1-D continuous sequence (raster-scan position alignment as illustrated in Fig. 3 (a)) and concatenated with instruction tokens for multimodal alignment. We note that such row-by-row positional alignment strategy is not natural for 2-D image data, as it breaks spatial continuity on column dimension. Due to the long-term decay in RoPE, information flow from visual token w_m to w_{m+1} differs from that to $w_{m+\sqrt{V}}$, which diverges from spatial locality of 2-D visual features.

Instead of adopting raster-scan sequential order, we design a concentric positional alignment strategy as illustrated in Fig. 3 (b). In our design, position m of visual tokens are organized in a form of 2D concentric square, which increases from the peripheral of 2-D inputs to the center. In comparison to sequence order of $\{1, 2, \dots, V\}$ for visual tokens \mathbb{S}_{vision} , such concentric positional alignment reduces relative distance between visual and instruction tokens $\mathbb{S}_{instruct}$. For a visual token sequence

of length V and a instruction token sequence of length T , the maximum distance between visual tokens \mathbb{S}_{vision} and instruction tokens $\mathbb{S}_{instruct}$ is $(\frac{\sqrt{V}}{2} + T - 1)$. This concentric sequential ordering also better maintains 2-D spatial locality of visual tokens. Under this scenario, visual tokens that are closer in euclidean distances are causally correlated when position m increases. Meanwhile, visual tokens that share the same position are correlated in visual self-attention. We note that such design mitigates negative effect from RoPE long-term decay, via decreasing relative distances between \mathbb{S}_{vision} and $\mathbb{S}_{instruct}$ while keeping causal inference scheme in pre-trained LLMs like LLaMA [64].

Concentric Causal Masking. Another part of our method resorts to modification of default causal attention masking towards our concentric visual token reorganization. As presented in Fig. 3 (c), a query feature q_m (derived from w_m) only attends to preceding key features $k_{\leq m}$. Likewise for our method, we follow the same principle to force causal attention masking in 2-D visual inputs. We visualize our masking in Fig. 3 (d), where the total length of visual tokens are 36 (6 by 6). Combining visual token re-organization with concentric causal masking, our method models 2-D continuity for visual inputs and effectively mitigates the object hallucination issue brought by long-term decay in RoPE.

5 Experiments

We first describe training details for our position alignment approach and evaluation setups in Sec. 5.1. Subsequently, we report results for several popular benchmarks that demonstrates efficacy of our simple design in the remaining subsections. Further, we present qualitative comparison in Appendix D.2 where our approach generates less hallucinated responses. From a broader scope, we present that our positional alignment strategy benefits general perception capability of LVLMs, where preliminary experiments show that it surpasses the baseline consistently over six multimodal benchmarks [36, 28, 22, 48, 8, 49]. We refer to these results in Appendix D.1 due to page limits. By default, we conduct our training and evaluation with Vicuna-7B [11] model, unless otherwise stated.

5.1 Training Details

Following [46, 45], we adopt pre-trained CLIP ViT-L/14 [55] with 336x336 resolutions as visual encoder and Vicuna-7B [12] as LLM, and a 2-layer MLP that connects the visual encoder and LLM. Training consists of two stages, including 1) a pre-training over CC-558K dataset [46] with global batch size of 256 and 2) a instruction tuning with a 665k multi-turn conversation dataset [45] with global batch size of 128.

5.2 POPE

Polling-based Object Probing Evaluation (POPE) [41] is proposed to provide a detailed evaluation of object hallucination in LVLMs, by querying the models about presence of specific objects in given images with yes-or-no questions. POPE adopts three sampling options to sample negative objects: random, popular and adversarial. We refer to [41] for these setups. Following [34], three datasets are included in our evaluation, including COCO [42], GQA [28] and A-OKVQA [58]. For each evaluation setup, every subset includes 3,000 questions for 500 images, which leads to 27,000 yes-or-no questions in total.

The experimental results are presented in Tab. 1. Our method achieves the highest accuracy and F1 scores across all datasets and negative sampling setups. By re-organization of visual tokens and concentric masking, our approach achieves 5.48%, 7.86% and 6.70% accuracy improvement and 5.89%, 7.71% and 6.19% F1 score improvement over the baseline model [46]. We also observe consistent and notable performance gains against state-of-the-art hallucination mitigation methods. CCA surpasses VCD [34] by 1.02%, 4.51% and 2.65% on three datasets. Particularly, we observe 3.09%, 5.01% and 3.59% F1 score improvement over adversarial evaluation set, which selects the most frequent co-occurring objects with ground-truth objects in image inputs, posing challenges for LVLMs to discern spurious correlation. Our trained model is also comparable to LLaVA-RLHF model (with Vicuna-13B as its LLM) [62] that additionally aligns model responses with human preference. These results indicate importance of re-organizing visual tokens in vision-language alignment.

Table 1: **POPE Results**. acc: accuracy. f1: f1 score, measured by precision and recall. Baseline and VCD results are reported by paper [34].

Evaluation	Method	random		popular		adversarial		average	
		acc	f1	acc	f1	acc	f1	acc	f1
MSCOCO [42]	baseline	83.29	81.33	81.88	80.06	78.96	77.57	81.38	79.65
	VCD [34]	87.73	87.16	85.38	85.06	80.88	81.33	84.66	84.52
	LLaVA-RLHF [62]	85.90	83.92	83.90	82.05	82.60	80.88	84.13	82.28
	CCA-LLaVA	88.03	86.65	86.87	85.54	85.67	84.42	86.86	85.54
A-OKVQA [58]	baseline	83.45	82.56	79.90	79.59	74.04	75.15	79.13	79.10
	VCD [34]	86.15	86.34	81.85	82.82	74.97	77.73	80.99	82.30
	LLaVA-RLHF [62]	87.67	86.60	85.20	84.34	79.97	79.92	84.28	83.62
	CCA-LLaVA	90.27	89.71	88.40	87.98	82.30	82.74	86.99	86.81
GQA [28]	baseline	83.73	82.95	78.17	78.37	75.08	76.06	78.99	79.13
	VCD [34]	86.65	86.99	80.73	82.24	76.09	78.78	81.16	82.67
	LLaVA-RLHF [62]	84.93	83.38	81.37	80.23	78.30	77.70	81.53	80.44
	CCA-LLaVA	88.40	87.68	86.47	85.91	82.20	82.37	85.69	85.32

5.3 CHAIR

We further evaluate our method on Caption Hallucination Assessment with Image Relevance (CHAIR) metric. CHAIR was a pioneering study introduced to measure object hallucination in image captioning [57]. It quantifies the factuality of a model by calculating the proportion of objects not present in ground truth over all objects in caption output. It contains both instance level score CHAIR_I (shorted for C_I) and sentence level score CHAIR_S (C_S) which holistically assess a model’s performance. Specifically, CHAIR metric is formulated as:

$$C_S = \frac{|\{\text{sentences with hallucinated objects}\}|}{|\{\text{all sentences}\}|}, \quad C_I = \frac{|\{\text{hallucinated objects}\}|}{|\{\text{all mentioned objects}\}|}$$

where lower scores corresponds to better performance. Following previous studies [26], we prompt LVLMs with “*Please describe this image in detail.*”. Note that LVLMs’s performance on CHAIR metric is highly dependent on their output sentence length. Short and succinct responses have less chances to make mistakes and thus would generally have better CHAIR scores. Different textual prompts such as “*in detail*” and “*in brief*” also influences output length and creates bias in CHAIR evaluation [41]. To offset the influence of output length and prompt phrasing and ensure fair basis of comparison, we follow the experimental setup in OPERA [26] and set the maximum text token to 64 and 512 respectively to examine hallucination on both short and long responses. Following [26], we sample 500 images from COCO VAL 2014 [42] to generate descriptions from different models and hallucination mitigation methods.

Our image caption evaluation result on CHAIR is shown in Tab. 2. For greedy decoding, our model surpasses baseline model [46] by 3.2% while maintaining high object recall (80.3% v.s. 80.4%) for long-response generation (by setting max new tokens to 512). Note that longer textual responses suggests more significant distance between visual and instruction tokens, leading to higher hallucination rates [83], which can be improved by our approach that reduces relative distance between visual and textual tokens. Our results are comparable against LLaVA-RLHF [62] over this setup. On short responses, our model also outperforms baseline model by 2.8% on sentence-level and 0.8% on instance-level while maintaining high object recall.

Our approach is also effective when using beam search for autoregressive decoding. We surpass the baseline by 0.8% and 0.5% on long-response generation, and 2.2% and 0.5% on short-response generation for C_S and C_I , respectively. Our approach is also complementary to OPERA [26]. In comparison to baseline model that using OPERA decoding, our approach are 1.8% and 1.1% better for C_S and C_I on long-response setting. We observe consistent performance gains in short-response generation (1.6% for C_S and 0.9% for C_I). Quantitative evaluations on open-ended generation indicates importance of a better positional alignment strategy and efficacy of our design.

Table 2: **CHAIR results**. For evaluation setups, 512 and 64 refer to a hyperparameter that relates to the length of LVLM responses, corresponding to long-text and short-text generation, respectively.

Evaluation	Method	512				64			
		C_{\downarrow}^S	C_{\downarrow}^I	rec_{\uparrow}	len	C_{\downarrow}^S	C_{\downarrow}^I	rec_{\uparrow}	len
<i>greedy</i>	baseline	46.2	12.9	80.3	97.2	21.0	6.2	66.3	54.9
	LLaVA-RLHF [62]	43.6	10.5	78.0	117.9	19.6	5.4	64.9	54.0
	CCA-LLaVA	43.0	11.5	80.4	96.6	18.2	5.4	66.7	54.5
<i>beam</i> (5)	baseline	49.4	13.9	79.9	96.1	18.2	5.8	64.0	52.7
	OPERA [26]	46.8	13.4	79.6	93.2	17.8	5.9	64.3	53.0
	CCA-LLaVA	48.6	13.4	79.9	94.2	16.0	5.3	64.8	52.7
	CCA-LLaVA + OPERA [26]	45.0	12.3	79.5	91.8	16.2	5.0	65.0	52.9

5.4 MME

The MME hallucination subset extends scope beyond object hallucination. Following [34], we evaluate 4 perception sub-tasks that examines LVLMs on object-level and attribute-level hallucinations, including measure of object existence, count, position and color. As presented in Tab. 3, our method surpasses the baseline by 76.33 on these tasks. In comparison to previous hallucination mitigation method VCD, our approach demonstrates non-negligible performance gains over all subtasks (e.g., 2.00 improvement from VCD v.s. 24.00 improvement from our method). These results indicate the potential of CCA to improve general perception capability of LVLMs.

Table 3: MME results.

Model	Object-level existence	Object-level count	Attribute-level position	Attribute-level color	Total
baseline	175.67	124.67	114.00	151.00	565.33
OPERA [26]	180.67	133.33	123.33	155.00	592.33
VCD [34]	184.66	138.33	128.67	153.00	604.66
CCA-LLaVA	190.00	148.33	128.33	175.00	641.66

Table 4: LLaVA Bench (In-the-Wild) results.

Model	Complex	Detail	Conv	Overall
baseline	65.8	51.2	54.6	58.9
OPERA [26]	66.4	56.9	44.0	61.3
VCD [34]	69.6	51.8	57.3	61.6
CCA-LLaVA	66.1	53.9	69.4	64.3

5.5 GPT4V-Aided Evaluation

We also evaluate our approach on LLaVA-Bench (In-the-Wild) [46], composed of 24 images with 60 questions in total. LLaVA-Bench (In-the-Wild) constitutes three types of questions, including conversation, detailed description and complex reasoning. Following [46, 26], we ask these models to generate responses and let the text-only GPT-4 [1] be the judge to rate these responses. The results are presented in Tab. 4. In comparison to OPERA [26] that specializes in open-ended generation, our method still stands out when examined by GPT-4 according to detailness and correctness, suggesting efficacy of our positional alignment strategy on generating accurate long responses.

6 Conclusion and Limitations

In this paper, we aim to mitigate object hallucination in Large Vision-Language Model (LVLM). We perform in-depth analysis on correlation between object hallucination and Rotary Position Encoding, a widely used positional dependency modeling design in existing LVLMs. We find that LVLMs are more likely to hallucinate when relevant visual cues are distant from instruction tokens in 1-D multimodal sequence, due to long-term decay in RoPE. To this end, we propose Concentric Causal Attention, a simple yet effective positional alignment strategy that reduces relative distances between visual and instruction tokens, alleviating negative impact brought by RoPE long decay on object hallucination. Experimental results over multiple evaluation benchmarks supports our design, indicating importance of better position alignment strategy.

Limitation. While this study shows improvements on mitigating object hallucination in LVLMs, our focus is only limited to handling of image-text inputs. We consider positional alignment strategy for other modalities of input data as future works, such as audio or video inputs that differs from image-text modalities.

Acknowledgments and Disclosure of Funding

This project is funded by the Ministry of Education Singapore, under Tier-1 project scheme with project number RG18/22 and Tier-2 project scheme with project number MOE-T2EP20220-0003.

References

- [1] Josh Achiam, Steven Adler, Sandhini Agarwal, Lama Ahmad, Ilge Akkaya, Florencia Leoni Aleman, Diogo Almeida, Janko Altenschmidt, Sam Altman, Shyamal Anadkat, et al. Gpt-4 technical report. *arXiv preprint arXiv:2303.08774*, 2023.
- [2] Jean-Baptiste Alayrac, Jeff Donahue, Pauline Luc, Antoine Miech, Iain Barr, Yana Hasson, Karel Lenc, Arthur Mensch, Katherine Millican, Malcolm Reynolds, et al. Flamingo: a visual language model for few-shot learning. *Advances in Neural Information Processing Systems*, 35:23716–23736, 2022.
- [3] Wenbin An, Feng Tian, Sicong Leng, Jiahao Nie, Haonan Lin, QianYing Wang, Guang Dai, Ping Chen, and Shijian Lu. Agla: Mitigating object hallucinations in large vision-language models with assembly of global and local attention. *arXiv preprint arXiv:2406.12718*, 2024.
- [4] Anas Awadalla, Irena Gao, Josh Gardner, Jack Hessel, Yusuf Hanafy, Wanrong Zhu, Kalyani Marathe, Yonatan Bitton, Samir Gadre, Shiori Sagawa, et al. Openflamingo: An open-source framework for training large autoregressive vision-language models. *arXiv preprint arXiv:2308.01390*, 2023.
- [5] Jinze Bai, Shuai Bai, Shusheng Yang, Shijie Wang, Sinan Tan, Peng Wang, Junyang Lin, Chang Zhou, and Jingren Zhou. Qwen-vl: A versatile vision-language model for understanding, localization, text reading, and beyond. *arXiv preprint arXiv:2402.16050*, 2023.
- [6] Junbum Cha, Wooyoung Kang, Jonghwan Mun, and Byungseok Roh. Honeybee: Locality-enhanced projector for multimodal llm. *arXiv preprint arXiv:2312.06742*, 2023.
- [7] Keqin Chen, Zhao Zhang, Weili Zeng, Richong Zhang, Feng Zhu, and Rui Zhao. Shikra: Unleashing multimodal llm’s referential dialogue magic. *arXiv preprint arXiv:2306.15195*, 2023.
- [8] Lin Chen, Jinsong Li, Xiaoyi Dong, Pan Zhang, Yuhang Zang, Zehui Chen, Haodong Duan, Jiaqi Wang, Yu Qiao, Dahua Lin, et al. Are we on the right way for evaluating large vision-language models? *arXiv preprint arXiv:2403.20330*, 2024.
- [9] Wei-Ge Chen, Irina Spiridonova, Jianwei Yang, Jianfeng Gao, and Chunyuan Li. Llava-interactive: An all-in-one demo for image chat, segmentation, generation and editing. *arXiv preprint arXiv:2311.00571*, 2023.
- [10] Zhaorun Chen, Zhuokai Zhao, Hongyin Luo, Huaxiu Yao, Bo Li, and Jiawei Zhou. Halc: Object hallucination reduction via adaptive focal-contrast decoding. *arXiv preprint arXiv:2403.00425*, 2024.
- [11] Wei-Lin Chiang, Zhuohan Li, Zi Lin, Ying Sheng, Zhanghao Wu, Hao Zhang, Lianmin Zheng, Siyuan Zhuang, Yonghao Zhuang, Joseph E Gonzalez, et al. Vicuna: An open-source chatbot impressing gpt-4 with 90%* chatgpt quality. See <https://vicuna.lmsys.org> (accessed 14 April 2023), 2023.
- [12] Wei-Lin Chiang, Zhuohan Li, Zi Lin, Ying Sheng, Zhanghao Wu, Hao Zhang, Lianmin Zheng, Siyuan Zhuang, Yonghao Zhuang, Joseph E. Gonzalez, Ion Stoica, and Eric P. Xing. Vicuna: An open-source chatbot impressing gpt-4 with 90%* chatgpt quality, March 2023.
- [13] Xiangxiang Chu, Jianlin Su, Bo Zhang, and Chunhua Shen. Visionllama: A unified llama interface for vision tasks. *arXiv preprint arXiv:2403.00522*, 2024.
- [14] Chenhang Cui, Yiyang Zhou, Xinyu Yang, Shirley Wu, Linjun Zhang, James Zou, and Huaxiu Yao. Holistic analysis of hallucination in gpt-4v (ision): Bias and interference challenges. *arXiv preprint arXiv:2311.03287*, 2023.
- [15] Wenliang Dai, Junnan Li, Dongxu Li, Anthony Meng Huat Tiong, Junqi Zhao, Weisheng Wang, Boyang Li, Pascale N Fung, and Steven Hoi. Instructblip: Towards general-purpose vision-language models with instruction tuning. *Advances in Neural Information Processing Systems*, 36, 2024.
- [16] Jia Deng, Wei Dong, Richard Socher, Li-Jia Li, Kai Li, and Li Fei-Fei. Imagenet: A large-scale hierarchical image database. In *2009 IEEE conference on computer vision and pattern recognition*, pages 248–255. Ieee, 2009.

[17] Jacob Devlin, Ming-Wei Chang, Kenton Lee, and Kristina Toutanova. Bert: Pre-training of deep bidirectional transformers for language understanding. *arXiv preprint arXiv:1810.04805*, 2018.

[18] Alexey Dosovitskiy, Lucas Beyer, Alexander Kolesnikov, Dirk Weissenborn, Xiaohua Zhai, Thomas Unterthiner, Mostafa Dehghani, Matthias Minderer, Georg Heigold, Sylvain Gelly, et al. An image is worth 16x16 words: Transformers for image recognition at scale. *arXiv preprint arXiv:2010.11929*, 2020.

[19] Alessandro Favero, Luca Zancato, Matthew Trager, Siddharth Choudhary, Pramuditha Perera, Alessandro Achille, Ashwin Swaminathan, and Stefano Soatto. Multi-modal hallucination control by visual information grounding. In *Proceedings of the IEEE/CVF Conference on Computer Vision and Pattern Recognition*, pages 14303–14312, 2024.

[20] Chaoyou Fu, Peixian Chen, Yunhang Shen, Yulei Qin, Mengdan Zhang, Xu Lin, Jinrui Yang, Xiawu Zheng, Ke Li, Xing Sun, et al. Mme: A comprehensive evaluation benchmark for multimodal large language models. *arXiv preprint arXiv:2306.13394*, 2023.

[21] Tianrui Guan, Fuxiao Liu, Xiyang Wu, Ruiqi Xian, Zongxia Li, Xiaoyu Liu, Xijun Wang, Lichang Chen, Furong Huang, Yaser Yacoob, et al. Hallusionbench: An advanced diagnostic suite for entangled language hallucination & visual illusion in large vision-language models. *arXiv preprint arXiv:2310.14566*, 2023.

[22] Danna Gurari, Qing Li, Abigale J Stangl, Anhong Guo, Chi Lin, Kristen Grauman, Jiebo Luo, and Jeffrey P Bigham. Vizwiz grand challenge: Answering visual questions from blind people. In *Proceedings of the IEEE conference on computer vision and pattern recognition*, pages 3608–3617, 2018.

[23] Pengcheng He, Xiaodong Liu, Jianfeng Gao, and Weizhu Chen. Deberta: Decoding-enhanced bert with disentangled attention. *arXiv preprint arXiv:2006.03654*, 2020.

[24] Sepp Hochreiter and Jürgen Schmidhuber. Long short-term memory. *Neural computation*, 9(8):1735–1780, 1997.

[25] Edward J Hu, Yelong Shen, Phillip Wallis, Zeyuan Allen-Zhu, Yuanzhi Li, Shean Wang, Lu Wang, and Weizhu Chen. Lora: Low-rank adaptation of large language models. *arXiv preprint arXiv:2106.09685*, 2021.

[26] Qidong Huang, Xiaoyi Dong, Pan Zhang, Bin Wang, Conghui He, Jiaqi Wang, Dahua Lin, Weiming Zhang, and Nenghai Yu. Opera: Alleviating hallucination in multi-modal large language models via over-trust penalty and retrospection-allocation. *arXiv preprint arXiv:2311.17911*, 2023.

[27] Zhiheng Huang, Davis Liang, Peng Xu, and Bing Xiang. Improve transformer models with better relative position embeddings. *arXiv preprint arXiv:2009.13658*, 2020.

[28] Drew A Hudson and Christopher D Manning. Gqa: A new dataset for real-world visual reasoning and compositional question answering. In *Proceedings of the IEEE/CVF conference on computer vision and pattern recognition*, pages 6700–6709, 2019.

[29] Chaoya Jiang, Haiyang Xu, Mengfan Dong, Jiaxing Chen, Wei Ye, Ming Yan, Qinghao Ye, Ji Zhang, Fei Huang, and Shikun Zhang. Hallucination augmented contrastive learning for multimodal large language model. *arXiv preprint arXiv:2312.06968*, 2023.

[30] Dongfu Jiang, Xuan He, Huaye Zeng, Con Wei, Max Ku, Qian Liu, and Wenhui Chen. Mantis: Interleaved multi-image instruction tuning. *arXiv preprint arXiv:2405.01483*, 2024.

[31] Guolin Ke, Di He, and Tie-Yan Liu. Rethinking positional encoding in language pre-training. *arXiv preprint arXiv:2006.15595*, 2020.

[32] Xin Lai, Zhuotao Tian, Yukang Chen, Yanwei Li, Yuhui Yuan, Shu Liu, and Jiaya Jia. Lisa: Reasoning segmentation via large language model. *arXiv preprint arXiv:2308.00692*, 2023.

[33] Seongyun Lee, Sue Hyun Park, Yongrae Jo, and Minjoon Seo. Volcano: mitigating multimodal hallucination through self-feedback guided revision. *arXiv preprint arXiv:2311.07362*, 2023.

[34] Sicong Leng, Hang Zhang, Guanzheng Chen, Xin Li, Shijian Lu, Chunyan Miao, and Lidong Bing. Mitigating object hallucinations in large vision-language models through visual contrastive decoding. *arXiv preprint arXiv:2311.16922*, 2023.

[35] Bo Li, Yuanhan Zhang, Liangyu Chen, Jinghao Wang, Jingkang Yang, and Ziwei Liu. Otter: A multi-modal model with in-context instruction tuning. *arXiv preprint arXiv:2305.03726*, 2023.

[36] Bohao Li, Rui Wang, Guangzhi Wang, Yuying Ge, Yixiao Ge, and Ying Shan. Seed-bench: Benchmarking multimodal llms with generative comprehension. *arXiv preprint arXiv:2307.16125*, 2023.

[37] Junnan Li, Dongxu Li, Silvio Savarese, and Steven Hoi. Blip-2: Bootstrapping language-image pre-training with frozen image encoders and large language models. In *International conference on machine learning*, pages 19730–19742. PMLR, 2023.

[38] Junnan Li, Dongxu Li, Caiming Xiong, and Steven Hoi. Blip: Bootstrapping language-image pre-training for unified vision-language understanding and generation. In *International conference on machine learning*, pages 12888–12900. PMLR, 2022.

[39] Kunchang Li, Yali Wang, Yinan He, Yizhuo Li, Yi Wang, Yi Liu, Zun Wang, Jilan Xu, Guo Chen, Ping Luo, et al. Mvbench: A comprehensive multi-modal video understanding benchmark. *arXiv preprint arXiv:2311.17005*, 2023.

[40] Yanwei Li, Yuechen Zhang, Chengyao Wang, Zhisheng Zhong, Yixin Chen, Ruihang Chu, Shaoteng Liu, and Jiaya Jia. Mini-gemini: Mining the potential of multi-modality vision language models. *arXiv preprint arXiv:2403.18814*, 2024.

[41] Yifan Li, Yifan Du, Kun Zhou, Jinpeng Wang, Wayne Xin Zhao, and Ji-Rong Wen. Evaluating object hallucination in large vision-language models. *arXiv preprint arXiv:2305.10355*, 2023.

[42] Tsung-Yi Lin, Michael Maire, Serge Belongie, James Hays, Pietro Perona, Deva Ramanan, Piotr Dollár, and C Lawrence Zitnick. Microsoft coco: Common objects in context. In *Computer Vision–ECCV 2014: 13th European Conference, Zurich, Switzerland, September 6–12, 2014, Proceedings, Part V 13*, pages 740–755. Springer, 2014.

[43] Fuxiao Liu, Kevin Lin, Linjie Li, Jianfeng Wang, Yaser Yacoob, and Lijuan Wang. Mitigating hallucination in large multi-modal models via robust instruction tuning. In *The Twelfth International Conference on Learning Representations*, 2024.

[44] Hanchao Liu, Wenyuan Xue, Yifei Chen, Dapeng Chen, Xiutian Zhao, Ke Wang, Liping Hou, Rongjun Li, and Wei Peng. A survey on hallucination in large vision-language models. *arXiv preprint arXiv:2402.00253*, 2024.

[45] Haotian Liu, Chunyuan Li, Yuheng Li, and Yong Jae Lee. Improved baselines with visual instruction tuning. *arXiv preprint arXiv:2310.03744*, 2023.

[46] Haotian Liu, Chunyuan Li, Qingyang Wu, and Yong Jae Lee. Visual instruction tuning. *Advances in neural information processing systems*, 36, 2024.

[47] Shilong Liu, Zhaoyang Zeng, Tianhe Ren, Feng Li, Hao Zhang, Jie Yang, Chunyuan Li, Jianwei Yang, Hang Su, Jun Zhu, et al. Grounding dino: Marrying dino with grounded pre-training for open-set object detection. *arXiv preprint arXiv:2303.05499*, 2023.

[48] Yuan Liu, Haodong Duan, Yuanhan Zhang, Bo Li, Songyang Zhang, Wangbo Zhao, Yike Yuan, Jiaqi Wang, Conghui He, Ziwei Liu, et al. Mmbench: Is your multi-modal model an all-around player? *arXiv preprint arXiv:2307.06281*, 2023.

[49] Pan Lu, Swaroop Mishra, Tanglin Xia, Liang Qiu, Kai-Wei Chang, Song-Chun Zhu, Oyvind Tafjord, Peter Clark, and Ashwin Kalyan. Learn to explain: Multimodal reasoning via thought chains for science question answering. *Advances in Neural Information Processing Systems*, 35:2507–2521, 2022.

[50] Zeyu Lu, Zidong Wang, Di Huang, Chengyue Wu, Xihui Liu, Wanli Ouyang, and Lei Bai. Fit: Flexible vision transformer for diffusion model. *arXiv preprint arXiv:2402.12376*, 2024.

[51] Fan Ma, Xiaojie Jin, Heng Wang, Yuchen Xian, Jiashi Feng, and Yi Yang. Vista-llama: Reliable video narrator via equal distance to visual tokens. *arXiv preprint arXiv:2312.08870*, 2023.

[52] Jiahao Nie, Gongjie Zhang, Wenbin An, Yap-Peng Tan, Alex C Kot, and Shijian Lu. Mmrel: A relation understanding dataset and benchmark in the mllm era. *arXiv preprint arXiv:2406.09121*, 2024.

[53] Bowen Peng, Jeffrey Quesnelle, Honglu Fan, and Enrico Shippole. Yarn: Efficient context window extension of large language models. *arXiv preprint arXiv:2309.00071*, 2023.

[54] Zhiliang Peng, Wenhui Wang, Li Dong, Yaru Hao, Shaohan Huang, Shuming Ma, and Furu Wei. Kosmos-2: Grounding multimodal large language models to the world. *arXiv preprint arXiv:2306.14824*, 2023.

[55] Alec Radford, Jong Wook Kim, Chris Hallacy, Aditya Ramesh, Gabriel Goh, Sandhini Agarwal, Girish Sastry, Amanda Askell, Pamela Mishkin, Jack Clark, et al. Learning transferable visual models from natural language supervision. In *International conference on machine learning*, pages 8748–8763. PMLR, 2021.

[56] Colin Raffel, Noam Shazeer, Adam Roberts, Katherine Lee, Sharan Narang, Michael Matena, Yanqi Zhou, Wei Li, and Peter J Liu. Exploring the limits of transfer learning with a unified text-to-text transformer. *Journal of machine learning research*, 21(140):1–67, 2020.

[57] Anna Rohrbach, Lisa Anne Hendricks, Kaylee Burns, Trevor Darrell, and Kate Saenko. Object hallucination in image captioning. *arXiv preprint arXiv:1809.02156*, 2018.

[58] Dustin Schwenk, Apoorv Khandelwal, Christopher Clark, Kenneth Marino, and Roozbeh Mottaghi. A-ovqa: A benchmark for visual question answering using world knowledge. In *European Conference on Computer Vision*, pages 146–162. Springer, 2022.

[59] Peter Shaw, Jakob Uszkoreit, and Ashish Vaswani. Self-attention with relative position representations. *arXiv preprint arXiv:1803.02155*, 2018.

[60] Amanpreet Singh, Vivek Natarajan, Meet Shah, Yu Jiang, Xinlei Chen, Dhruv Batra, Devi Parikh, and Marcus Rohrbach. Towards vqa models that can read. In *Proceedings of the IEEE/CVF conference on computer vision and pattern recognition*, pages 8317–8326, 2019.

[61] Jianlin Su, Murtadha Ahmed, Yu Lu, Shengfeng Pan, Wen Bo, and Yunfeng Liu. Roformer: Enhanced transformer with rotary position embedding. *Neurocomputing*, 568:127063, 2024.

[62] Zhiqing Sun, Sheng Shen, Shengcao Cao, Haotian Liu, Chunyuan Li, Yikang Shen, Chuang Gan, Liang Yan Gui, Yu-Xiong Wang, Yiming Yang, et al. Aligning large multimodal models with factually augmented rlhf. *arXiv preprint arXiv:2309.14525*, 2023.

[63] Hugo Touvron, Thibaut Lavril, Gautier Izacard, Xavier Martinet, Marie-Anne Lachaux, Timothée Lacroix, Baptiste Rozière, Naman Goyal, Eric Hambro, Faisal Azhar, et al. Llama: Open and efficient foundation language models. *arXiv preprint arXiv:2302.13971*, 2023.

[64] Hugo Touvron, Louis Martin, Kevin Stone, Peter Albert, Amjad Almahairi, Yasmine Babaei, Nikolay Bashlykov, Soumya Batra, Prajjwal Bhargava, Shruti Bhosale, et al. Llama 2: Open foundation and fine-tuned chat models. *arXiv preprint arXiv:2307.09288*, 2023.

[65] Ashish Vaswani, Noam Shazeer, Niki Parmar, Jakob Uszkoreit, Llion Jones, Aidan N Gomez, Łukasz Kaiser, and Illia Polosukhin. Attention is all you need. *Advances in neural information processing systems*, 30, 2017.

[66] Junyang Wang, Yuhang Wang, Guohai Xu, Jing Zhang, Yukai Gu, Haitao Jia, Ming Yan, Ji Zhang, and Jitao Sang. An llm-free multi-dimensional benchmark for mllms hallucination evaluation. *arXiv preprint arXiv:2311.07397*, 2023.

[67] Weihan Wang, Qingsong Lv, Wenmeng Yu, Wenyi Hong, Ji Qi, Yan Wang, Junhui Ji, Zhuoyi Yang, Lei Zhao, Xixuan Song, et al. Cogvilm: Visual expert for pretrained language models. *arXiv preprint arXiv:2311.03079*, 2023.

[68] Xiyao Wang, Yuhang Zhou, Xiaoyu Liu, Hongjin Lu, Yuancheng Xu, Feihong He, Jaehong Yoon, Taixi Lu, Gedas Bertasius, Mohit Bansal, et al. Mementos: A comprehensive benchmark for multimodal large language model reasoning over image sequences. *arXiv preprint arXiv:2401.10529*, 2024.

[69] Yuxuan Wang, Yueqian Wang, Pengfei Wu, Jianxin Liang, Dongyan Zhao, and Zilong Zheng. Lstp: Language-guided spatial-temporal prompt learning for long-form video-text understanding. *arXiv preprint arXiv:2402.16050*, 2024.

[70] Junfei Wu, Qiang Liu, Ding Wang, Jinghao Zhang, Shu Wu, Liang Wang, and Tieniu Tan. Logical closed loop: Uncovering object hallucinations in large vision-language models. *arXiv preprint arXiv:2402.11622*, 2024.

[71] Qinghao Ye, Haiyang Xu, Guohai Xu, Jiabo Ye, Ming Yan, Yiyang Zhou, Junyang Wang, Anwen Hu, Pengcheng Shi, Yaya Shi, et al. mplug-owl: Modularization empowers large language models with multimodality. *arXiv preprint arXiv:2304.14178*, 2023.

[72] Shukang Yin, Chaoyou Fu, Sirui Zhao, Ke Li, Xing Sun, Tong Xu, and Enhong Chen. A survey on multimodal large language models. *arXiv preprint arXiv:2306.13549*, 2023.

- [73] Shukang Yin, Chaoyou Fu, Sirui Zhao, Tong Xu, Hao Wang, Dianbo Sui, Yunhang Shen, Ke Li, Xing Sun, and Enhong Chen. Woodpecker: Hallucination correction for multimodal large language models. *arXiv preprint arXiv:2310.16045*, 2023.
- [74] Haoxuan You, Haotian Zhang, Zhe Gan, Xianzhi Du, Bowen Zhang, Zirui Wang, Liangliang Cao, Shih-Fu Chang, and Yinfei Yang. Ferret: Refer and ground anything anywhere at any granularity. *arXiv preprint arXiv:2310.07704*, 2023.
- [75] Qifan Yu, Juncheng Li, Longhui Wei, Liang Pang, Wentao Ye, Bosheng Qin, Siliang Tang, Qi Tian, and Yueteng Zhuang. Hallucidocor: Mitigating hallucinatory toxicity in visual instruction data, 2023.
- [76] Tianyu Yu, Yuan Yao, Haoye Zhang, Taiwen He, Yifeng Han, Ganqu Cui, Jinyi Hu, Zhiyuan Liu, Hai-Tao Zheng, Maosong Sun, et al. Rlhf-v: Towards trustworthy mllms via behavior alignment from fine-grained correctional human feedback. *arXiv preprint arXiv:2312.00849*, 2023.
- [77] Yuqian Yuan, Wentong Li, Jian Liu, Dongqi Tang, Xinjie Luo, Chi Qin, Lei Zhang, and Jianke Zhu. Osprey: Pixel understanding with visual instruction tuning. *arXiv preprint arXiv:2312.10032*, 2023.
- [78] Zihao Yue, Liang Zhang, and Qin Jin. Less is more: Mitigating multimodal hallucination from an eos decision perspective, 2024.
- [79] Hang Zhang, Xin Li, and Lidong Bing. Video-llama: An instruction-tuned audio-visual language model for video understanding. *arXiv preprint arXiv:2306.02858*, 2023.
- [80] Kaichen Zhang, Bo Li, Peiyuan Zhang, Fanyi Pu, Joshua Adrian Cahyono, Kairui Hu, Shuai Liu, Yuanhan Zhang, Jingkang Yang, Chunyuan Li, et al. Lmms-eval: Reality check on the evaluation of large multimodal models. *arXiv preprint arXiv:2407.12772*, 2024.
- [81] Shilong Zhang, Peize Sun, Shoufa Chen, Min Xiao, Wenqi Shao, Wenwei Zhang, Kai Chen, and Ping Luo. Gpt4roi: Instruction tuning large language model on region-of-interest. *arXiv preprint arXiv:2307.03601*, 2023.
- [82] Yuechen Zhang, Shengju Qian, Bohao Peng, Shu Liu, and Jiaya Jia. Prompt highlighter: Interactive control for multi-modal llms. *arXiv preprint arXiv:2312.04302*, 2023.
- [83] Yiyang Zhou, Chenhang Cui, Jaehong Yoon, Linjun Zhang, Zhun Deng, Chelsea Finn, Mohit Bansal, and Huaxiu Yao. Analyzing and mitigating object hallucination in large vision-language models. In *The Twelfth International Conference on Learning Representations*, 2024.
- [84] Deyao Zhu, Jun Chen, Xiaoqian Shen, Xiang Li, and Mohamed Elhoseiny. Minigpt-4: Enhancing vision-language understanding with advanced large language models. *arXiv preprint arXiv:2304.10592*, 2023.
- [85] Ke Zhu, Liang Zhao, Zheng Ge, and Xiangyu Zhang. Self-supervised visual preference alignment. *arXiv preprint arXiv:2404.10501*, 2024.

Appendix

A Broader Impact

Like other LVLMs, models trained by our CCA approach have their potential benefits and risks when they are publicly released. As our approach is validated on LLaVA which constitutes CLIP, Vicuna and LLaMA, our trained models may inherit risks from these pre-trained visual encoders and large language models, including handling malicious inputs, hallucination or potential biases. We mitigate these issues following other LVLMs.

B RoPE in LLaMA

We further clarify the role of Rotary Position Encoding (RoPE) [61] in LLaMA architecture with a separate illustration. As Fig. 4 shows, RoPE is densely involved in LLaMA [63, 64], namely in all self-attention layers. This is architecturally distinct from how positions are involved in ViT, where absolute PEs are only added once right after patch embedding layer. As most open-source LVLMs are using LLaMA as their language backbones [46, 84, 15, 67, 30, 79], it is noteworthy to study how RoPE may affect multimodal perception when we connect pretrained vision models (e.g., CLIP) with LLaMA.

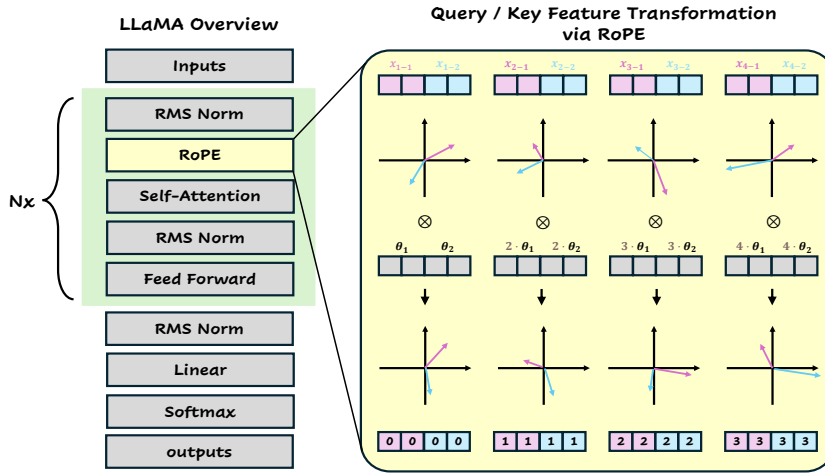


Figure 4: **RoPE in LLaMA**. A schematic view for LLaMA where RoPE is highlighted, and an example illustration on how RoPE is applied over query or key feature. We use a short input sequence with length of 4 and feature dimension of 4 for demonstration purpose. Input tokens are rotated with angles, subject to token positions. For mathematical definition, please refer to Sec. 3.

C Implementation Details

We include more details here about implementation for Fig. 1 and Fig. 2 results in main paper, including data and model architecture we use, and training details we follow.

C.1 Pilot Experiment

Training. As described in Sec. 3 of main paper, we train a baseline LVLM \mathcal{F}_b that follows raster-scan positional alignment and another LVLM \mathcal{F}_r that follows reversal raster-scan position alignment. For these two models, we carry out two-stage training following [46], except for the second stage we train both models for 20K steps with LoRA [25] due to resource limitations. Both experiments share the same training hyper-parameters as 665K full schedule training.

Inference. We sample 3,000 annotations from COCO VAL 2014 [42] to carry out our motivation experiments. For each annotation with its corresponding image, we crop an object according to its bounding box and paste it within a pre-defined template (a visually gray image), which is initialized with ImageNet [16] average pixel values. We test k spatial positions $\{v_1, \dots, v_k\}$, where k is set to 144, resulting in resolution of 12 by 12 for both aggregated results in Fig. 2. Workflow on how we construct such synthetic data is further presented in Fig. 5.



Figure 5: Workflow illustration on how we synthesize testing data. Given an image and box annotation for one object instance, we crop it and paste it on a template image, initialized with ImageNet mean pixel values. We paste every cropped region on every spatial position. Resulting data constitutes a large amount of questions about object existence, diverse in spatial positions.

C.2 Information Flow

We reveal long-term decay property of RoPE [61] in scope of LVLMs. To implement this, we use 3,000 image-query pairs from POPE [41] adversarial setup, and LLaVA-1.5-7B [46] as our LVLM. For each image-query pair, we extract and aggregate self-attentions from the first decoder layer of LLaMA [64]. We average obtained self-attentions across heads and images to obtain our quantitative results in Fig. 1. A pseudo code is provided below for further clarification.

```

def compute_vis_inst_flow(
    attn,
    img_token_pos,
    img_token_len
):
    """
    Return
        information flow from visual (vis) to instruction (inst) tokens.

    Input
        attn - self attentions.
        img_token_pos - where image sequence starts.
        img_token_len - sequence length for visual tokens.
    """
    inst_vis_attn = attn[
        ...
        ...
        img_token_pos + img_token_len + 1,
        img_token_pos: img_token_pos + img_token_len
    ]
    # average across images, heads, and instruction tokens.
    vis_inst_flow = inst_vis_attn.mean(dim=(0, 1, 2))
    return vis_inst_flow

```

D More Results

D.1 Comparison over Multiple-Choice Benchmarks

Beyond the scope of visual hallucination, we consider our proposed positional alignment as a general approach for improving perception capability for LVLMs. We further evaluate our trained model over six benchmarks that examines LVLMs general perception capability, including SEED-Bench [36], ScienceQA [49], GQA [28], Vizwiz [22], MMBench [48] and MMStar [8] which evaluates LVLMs perception capability with multiple choice questions. We use lmms-eval [80] to do our comparison.

For details of our evaluation benchmarks, SEED-Bench [36] consists of 19k multiple choice questions with human annotations, while spanning 12 evaluation dimensions, including both image and video data. MMBench [48] also examines LVLMs on general perception capabilities using a wide range of tasks. We also present our comparisons on ScienceQA [49], Vizwiz [22] and GQA [28] that examines certain perception capability, like knowledge and relation. Note that MMStar [8] is a vision-indispensable benchmark, which requires better visual grounding in trained LVLMs. We present our results against baseline model [46] in Tab. 5. In comparison to our baseline model LLaVA, our positional alignment approach achieves non-negligible gains across all six benchmarks, without introducing additional computation during training. Such performance gains highlight potential of Concentric Causal Attention on enhancing general visual perception capability of LVLMs.

Table 5: **Evaluation on Multiple-Choice Benchmarks.** Baseline results are reported by paper [45], except for MMStar reported by [8]. SEED^A, SEED^I and SEED^V refers to *all*, *image* and *video* evaluation, respectively. SeVa results are reported by [85].

Method	SEED ^A [36]	SEED ^I [36]	SEED ^V [36]	SQA [49]	GQA [28]	VizWiz [22]	MMBench [48]	MMStar [8]	TextVQA [60]
LLaVA [45]	58.6	66.1	37.3	66.8	62.0	50.0	64.3	30.0	58.2
LLaVA w/ VCD [34]	58.3	63.7	37.6	68.5	61.9	50.5	-	34.6	54.4
Seva-7b-dif [85]	-	65.8	-	67.5	60.7	-	65.6	-	-
Seva-7b-moco [85]	-	65.5	-	67.1	60.9	-	65.2	-	-
CCA-LLaVA (ours)	61.7	67.1	41.0	69.8	63.1	57.6	65.4	33.2	57.8

D.2 Qualitative Comparison

We present qualitative comparison between responses generated by baseline model [46] and our trained model. We show that baseline model are more likely to hallucinate, for example, bathtub and sink in Fig. 6, knife and cup in Fig. 7. We also show case study on LLaVA-Bench [46] as illustrated in Fig. 8, where baseline model hallucinates with object hat. We also note that baseline model hallucinates in optical character recognition and numbers as in Fig. 9, where our method mitigates these issues.

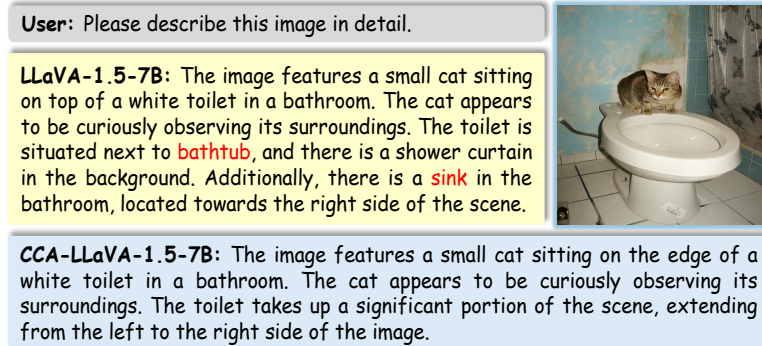


Figure 6: Qualitative comparison of open-ended generation between baseline and our method.

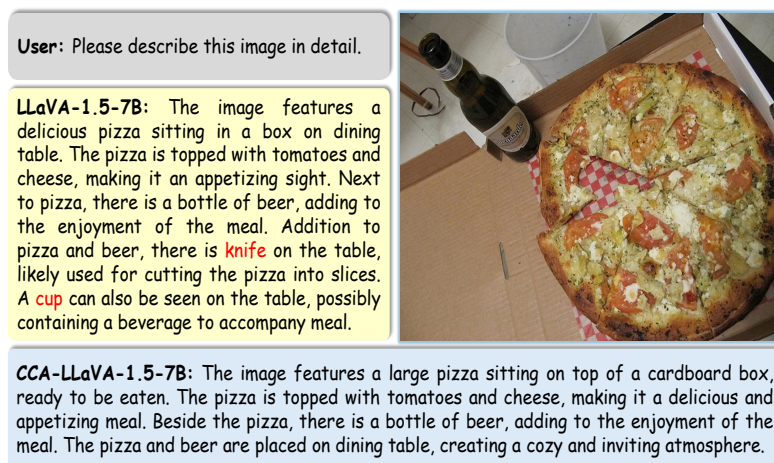


Figure 7: Qualitative comparison of open-ended generation between baseline and our method.

E Computation Resources

We use 4 NVIDIA RTX A6000s to train our models. Pre-training stage takes 12 hours while instruction tuning takes roughly 83 hours.

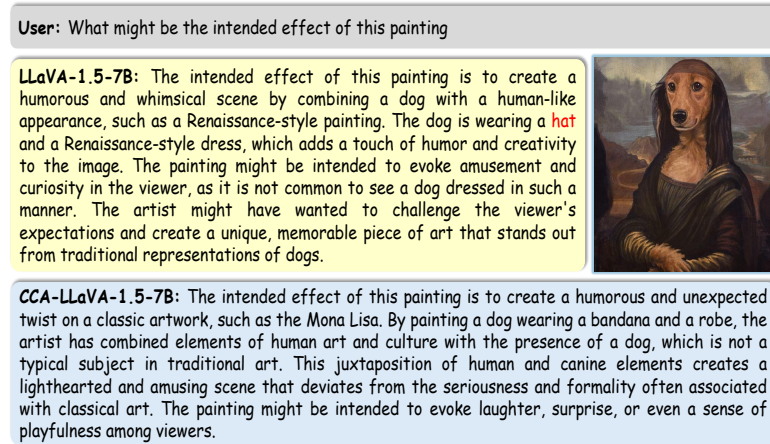


Figure 8: Case Study where question is sampled from LLaVA-Bench [46]. LLaVA hallucinates hat in its long response, while CCA answers correctly without hallucination.



Figure 9: Case Study where question is sampled from LLaVA-Bench [46]. CCA-LLaVA outperforms LLaVA on optical character recognition (left) and numerical prediction in given cases.

NeurIPS Paper Checklist

1. Claims

Question: Do the main claims made in the abstract and introduction accurately reflect the paper's contributions and scope?

Answer: [Yes]

Justification: The abstract and introduction clearly state the claims made in the paper. The claims match experimental results and reflect that our method can be expected to generalize to other settings.

Guidelines:

- The answer NA means that the abstract and introduction do not include the claims made in the paper.
- The abstract and/or introduction should clearly state the claims made, including the contributions made in the paper and important assumptions and limitations. A No or NA answer to this question will not be perceived well by the reviewers.
- The claims made should match theoretical and experimental results, and reflect how much the results can be expected to generalize to other settings.
- It is fine to include aspirational goals as motivation as long as it is clear that these goals are not attained by the paper.

2. Limitations

Question: Does the paper discuss the limitations of the work performed by the authors?

Answer: [Yes]

Justification: Please refer to Sec. 6 for limitations.

Guidelines:

- The answer NA means that the paper has no limitation while the answer No means that the paper has limitations, but those are not discussed in the paper.
- The authors are encouraged to create a separate "Limitations" section in their paper.
- The paper should point out any strong assumptions and how robust the results are to violations of these assumptions (e.g., independence assumptions, noiseless settings, model well-specification, asymptotic approximations only holding locally). The authors should reflect on how these assumptions might be violated in practice and what the implications would be.
- The authors should reflect on the scope of the claims made, e.g., if the approach was only tested on a few datasets or with a few runs. In general, empirical results often depend on implicit assumptions, which should be articulated.
- The authors should reflect on the factors that influence the performance of the approach. For example, a facial recognition algorithm may perform poorly when image resolution is low or images are taken in low lighting. Or a speech-to-text system might not be used reliably to provide closed captions for online lectures because it fails to handle technical jargon.
- The authors should discuss the computational efficiency of the proposed algorithms and how they scale with dataset size.
- If applicable, the authors should discuss possible limitations of their approach to address problems of privacy and fairness.
- While the authors might fear that complete honesty about limitations might be used by reviewers as grounds for rejection, a worse outcome might be that reviewers discover limitations that aren't acknowledged in the paper. The authors should use their best judgment and recognize that individual actions in favor of transparency play an important role in developing norms that preserve the integrity of the community. Reviewers will be specifically instructed to not penalize honesty concerning limitations.

3. Theory Assumptions and Proofs

Question: For each theoretical result, does the paper provide the full set of assumptions and a complete (and correct) proof?

Answer: [NA]

Justification: The paper does not include theoretical results.

Guidelines:

- The answer NA means that the paper does not include theoretical results.
- All the theorems, formulas, and proofs in the paper should be numbered and cross-referenced.
- All assumptions should be clearly stated or referenced in the statement of any theorems.

- The proofs can either appear in the main paper or the supplemental material, but if they appear in the supplemental material, the authors are encouraged to provide a short proof sketch to provide intuition.
- Inversely, any informal proof provided in the core of the paper should be complemented by formal proofs provided in appendix or supplemental material.
- Theorems and Lemmas that the proof relies upon should be properly referenced.

4. Experimental Result Reproducibility

Question: Does the paper fully disclose all the information needed to reproduce the main experimental results of the paper to the extent that it affects the main claims and/or conclusions of the paper (regardless of whether the code and data are provided or not)?

Answer: [Yes]

Justification: Please refer to Sec. 5.1 in the main text and Sec. C.1 for training our models.

Guidelines:

- The answer NA means that the paper does not include experiments.
- If the paper includes experiments, a No answer to this question will not be perceived well by the reviewers: Making the paper reproducible is important, regardless of whether the code and data are provided or not.
- If the contribution is a dataset and/or model, the authors should describe the steps taken to make their results reproducible or verifiable.
- Depending on the contribution, reproducibility can be accomplished in various ways. For example, if the contribution is a novel architecture, describing the architecture fully might suffice, or if the contribution is a specific model and empirical evaluation, it may be necessary to either make it possible for others to replicate the model with the same dataset, or provide access to the model. In general, releasing code and data is often one good way to accomplish this, but reproducibility can also be provided via detailed instructions for how to replicate the results, access to a hosted model (e.g., in the case of a large language model), releasing of a model checkpoint, or other means that are appropriate to the research performed.
- While NeurIPS does not require releasing code, the conference does require all submissions to provide some reasonable avenue for reproducibility, which may depend on the nature of the contribution. For example
 - (a) If the contribution is primarily a new algorithm, the paper should make it clear how to reproduce that algorithm.
 - (b) If the contribution is primarily a new model architecture, the paper should describe the architecture clearly and fully.
 - (c) If the contribution is a new model (e.g., a large language model), then there should either be a way to access this model for reproducing the results or a way to reproduce the model (e.g., with an open-source dataset or instructions for how to construct the dataset).
 - (d) We recognize that reproducibility may be tricky in some cases, in which case authors are welcome to describe the particular way they provide for reproducibility. In the case of closed-source models, it may be that access to the model is limited in some way (e.g., to registered users), but it should be possible for other researchers to have some path to reproducing or verifying the results.

5. Open access to data and code

Question: Does the paper provide open access to the data and code, with sufficient instructions to faithfully reproduce the main experimental results, as described in supplemental material?

Answer: [Yes]

Justification: We refer readers to <https://github.com/xing0047/cca-llava> for details of data and code guideline.

Guidelines:

- The answer NA means that paper does not include experiments requiring code.
- Please see the NeurIPS code and data submission guidelines (<https://nips.cc/public/guides/CodeSubmissionPolicy>) for more details.
- While we encourage the release of code and data, we understand that this might not be possible, so “No” is an acceptable answer. Papers cannot be rejected simply for not including code, unless this is central to the contribution (e.g., for a new open-source benchmark).
- The instructions should contain the exact command and environment needed to run to reproduce the results. See the NeurIPS code and data submission guidelines (<https://nips.cc/public/guides/CodeSubmissionPolicy>) for more details.

- The authors should provide instructions on data access and preparation, including how to access the raw data, preprocessed data, intermediate data, and generated data, etc.
- The authors should provide scripts to reproduce all experimental results for the new proposed method and baselines. If only a subset of experiments are reproducible, they should state which ones are omitted from the script and why.
- At submission time, to preserve anonymity, the authors should release anonymized versions (if applicable).
- Providing as much information as possible in supplemental material (appended to the paper) is recommended, but including URLs to data and code is permitted.

6. Experimental Setting/Details

Question: Does the paper specify all the training and test details (e.g., data splits, hyperparameters, how they were chosen, type of optimizer, etc.) necessary to understand the results?

Answer: **[Yes]**

Justification: Please refer to Sec. 5.1 in the main text for training details while Sec. 5 in the main text and Appendix D.1 for evaluation details.

Guidelines:

- The answer NA means that the paper does not include experiments.
- The experimental setting should be presented in the core of the paper to a level of detail that is necessary to appreciate the results and make sense of them.
- The full details can be provided either with the code, in appendix, or as supplemental material.

7. Experiment Statistical Significance

Question: Does the paper report error bars suitably and correctly defined or other appropriate information about the statistical significance of the experiments?

Answer: **[No]**

Justification: Error bars are not reported since training of LVLMs is computationally expensive.

Guidelines:

- The answer NA means that the paper does not include experiments.
- The authors should answer "Yes" if the results are accompanied by error bars, confidence intervals, or statistical significance tests, at least for the experiments that support the main claims of the paper.
- The factors of variability that the error bars are capturing should be clearly stated (for example, train/test split, initialization, random drawing of some parameter, or overall run with given experimental conditions).
- The method for calculating the error bars should be explained (closed form formula, call to a library function, bootstrap, etc.)
- The assumptions made should be given (e.g., Normally distributed errors).
- It should be clear whether the error bar is the standard deviation or the standard error of the mean.
- It is OK to report 1-sigma error bars, but one should state it. The authors should preferably report a 2-sigma error bar than state that they have a 96% CI, if the hypothesis of Normality of errors is not verified.
- For asymmetric distributions, the authors should be careful not to show in tables or figures symmetric error bars that would yield results that are out of range (e.g. negative error rates).
- If error bars are reported in tables or plots, The authors should explain in the text how they were calculated and reference the corresponding figures or tables in the text.

8. Experiments Compute Resources

Question: For each experiment, does the paper provide sufficient information on the computer resources (type of compute workers, memory, time of execution) needed to reproduce the experiments?

Answer: **[Yes]**

Justification: Please refer to Appendix E for GPUs we use and execution time for training LVLMs.

Guidelines:

- The answer NA means that the paper does not include experiments.
- The paper should indicate the type of compute workers CPU or GPU, internal cluster, or cloud provider, including relevant memory and storage.

- The paper should provide the amount of compute required for each of the individual experimental runs as well as estimate the total compute.
- The paper should disclose whether the full research project required more compute than the experiments reported in the paper (e.g., preliminary or failed experiments that didn't make it into the paper).

9. Code Of Ethics

Question: Does the research conducted in the paper conform, in every respect, with the NeurIPS Code of Ethics <https://neurips.cc/public/EthicsGuidelines>?

Answer: [\[Yes\]](#)

Justification: The research conducted in the paper conforms with the NeurIPS Code of Ethics.

Guidelines:

- The answer NA means that the authors have not reviewed the NeurIPS Code of Ethics.
- If the authors answer No, they should explain the special circumstances that require a deviation from the Code of Ethics.
- The authors should make sure to preserve anonymity (e.g., if there is a special consideration due to laws or regulations in their jurisdiction).

10. Broader Impacts

Question: Does the paper discuss both potential positive societal impacts and negative societal impacts of the work performed?

Answer: [\[Yes\]](#)

Justification: Please find Broader Impacts in Appendix A.

Guidelines:

- The answer NA means that there is no societal impact of the work performed.
- If the authors answer NA or No, they should explain why their work has no societal impact or why the paper does not address societal impact.
- Examples of negative societal impacts include potential malicious or unintended uses (e.g., disinformation, generating fake profiles, surveillance), fairness considerations (e.g., deployment of technologies that could make decisions that unfairly impact specific groups), privacy considerations, and security considerations.
- The conference expects that many papers will be foundational research and not tied to particular applications, let alone deployments. However, if there is a direct path to any negative applications, the authors should point it out. For example, it is legitimate to point out that an improvement in the quality of generative models could be used to generate deepfakes for disinformation. On the other hand, it is not needed to point out that a generic algorithm for optimizing neural networks could enable people to train models that generate Deepfakes faster.
- The authors should consider possible harms that could arise when the technology is being used as intended and functioning correctly, harms that could arise when the technology is being used as intended but gives incorrect results, and harms following from (intentional or unintentional) misuse of the technology.
- If there are negative societal impacts, the authors could also discuss possible mitigation strategies (e.g., gated release of models, providing defenses in addition to attacks, mechanisms for monitoring misuse, mechanisms to monitor how a system learns from feedback over time, improving the efficiency and accessibility of ML).

11. Safeguards

Question: Does the paper describe safeguards that have been put in place for responsible release of data or models that have a high risk for misuse (e.g., pretrained language models, image generators, or scraped datasets)?

Answer: [\[NA\]](#)

Justification: We use open-sourced models and data only. We have properly cited original papers of our training and evaluation data. The license for assets used in this paper are under CC-BY 4.0. Our models in this paper will be under CC-BY-NC-SA 4.0 license.

Guidelines:

- The answer NA means that the paper poses no such risks.
- Released models that have a high risk for misuse or dual-use should be released with necessary safeguards to allow for controlled use of the model, for example by requiring that users adhere to usage guidelines or restrictions to access the model or implementing safety filters.

- Datasets that have been scraped from the Internet could pose safety risks. The authors should describe how they avoided releasing unsafe images.
- We recognize that providing effective safeguards is challenging, and many papers do not require this, but we encourage authors to take this into account and make a best faith effort.

12. Licenses for existing assets

Question: Are the creators or original owners of assets (e.g., code, data, models), used in the paper, properly credited and are the license and terms of use explicitly mentioned and properly respected?

Answer: [Yes]

Justification: We have properly cited original papers of our training and evaluation data. The licenses for models we use include CLIP, which is under MIT License, and LLaMA2, which is under Apache-2.0.

Guidelines:

- The answer NA means that the paper does not use existing assets.
- The authors should cite the original paper that produced the code package or dataset.
- The authors should state which version of the asset is used and, if possible, include a URL.
- The name of the license (e.g., CC-BY 4.0) should be included for each asset.
- For scraped data from a particular source (e.g., website), the copyright and terms of service of that source should be provided.
- If assets are released, the license, copyright information, and terms of use in the package should be provided. For popular datasets, paperswithcode.com/datasets has curated licenses for some datasets. Their licensing guide can help determine the license of a dataset.
- For existing datasets that are re-packaged, both the original license and the license of the derived asset (if it has changed) should be provided.
- If this information is not available online, the authors are encouraged to reach out to the asset's creators.

13. New Assets

Question: Are new assets introduced in the paper well documented and is the documentation provided alongside the assets?

Answer: [NA]

Justification: The paper does not release new assets.

Guidelines:

- The answer NA means that the paper does not release new assets.
- Researchers should communicate the details of the dataset/code/model as part of their submissions via structured templates. This includes details about training, license, limitations, etc.
- The paper should discuss whether and how consent was obtained from people whose asset is used.
- At submission time, remember to anonymize your assets (if applicable). You can either create an anonymized URL or include an anonymized zip file.

14. Crowdsourcing and Research with Human Subjects

Question: For crowdsourcing experiments and research with human subjects, does the paper include the full text of instructions given to participants and screenshots, if applicable, as well as details about compensation (if any)?

Answer: [NA]

Justification: This paper does not involve crowdsourcing nor research with human subjects.

Guidelines:

- The answer NA means that the paper does not involve crowdsourcing nor research with human subjects.
- Including this information in the supplemental material is fine, but if the main contribution of the paper involves human subjects, then as much detail as possible should be included in the main paper.
- According to the NeurIPS Code of Ethics, workers involved in data collection, curation, or other labor should be paid at least the minimum wage in the country of the data collector.

15. Institutional Review Board (IRB) Approvals or Equivalent for Research with Human Subjects

Question: Does the paper describe potential risks incurred by study participants, whether such risks were disclosed to the subjects, and whether Institutional Review Board (IRB) approvals (or an equivalent approval/review based on the requirements of your country or institution) were obtained?

Answer: [NA]

Justification: The paper does not involve crowdsourcing nor research with human subjects.

Guidelines:

- The answer NA means that the paper does not involve crowdsourcing nor research with human subjects.
- Depending on the country in which research is conducted, IRB approval (or equivalent) may be required for any human subjects research. If you obtained IRB approval, you should clearly state this in the paper.
- We recognize that the procedures for this may vary significantly between institutions and locations, and we expect authors to adhere to the NeurIPS Code of Ethics and the guidelines for their institution.
- For initial submissions, do not include any information that would break anonymity (if applicable), such as the institution conducting the review.